Coordination-Induced Bond Weakening and Electrocatalytic Proton-Coupled Electron Transfer of a Ruthenium Verdazyl Complex

Conor M. Galvin, Daniel P. Marron, Julia M. Dressel, Robert M. Waymouth*

Department of Chemistry, Stanford University, Stanford CA 94305, United States

ABSTRACT

Coordination of the leucoverdazyl ligand 2,4-diisopropyl-6-(pyridin-2-yl)-1,4-dihydro-1,2,4,5-tetrazin-3(2H)-one **VdH** to Ru significantly weakens the ligand's N-H bond. Electrochemical measurements show that the metalated leucoverdazyl Ru(**VdH**)(acetylacetonate)₂ **RuVdH** has a lower pK_a(-5 units), BDFE (-7 kcal/mol), and hydricity (-22 kcal/mol) than the free ligand. DFT calculations suggest that the increased acidity is in part attributable to the stabilization of the conjugate base **Vd**⁻. When free, **Vd**⁻ distorts to avoid an $8\pi e^-$ antiaromatic state, but it remains planar when bound to Ru. Proton-coupled electron transfer (PCET) behavior is observed for both the free and metalated leucoverdazyls. PCET equilibrium between **Vd** radical and TEMPOH affords a **VdH** BDFE that is in good agreement with that obtained from electrochemical methods. **RuVd** exhibits electrocatalytic PCET donor behavior. Under acidic conditions, it reduces the persistent trityl radical ·CAr₃ (Ar = *p*-tert-butylphenyl) to the corresponding triarylmethane HCAr₃ via net 1e⁻/1H⁺ transfer from **RuVdH**.

INTRODUCTION

Coordination of ligands or small molecule substrates to metal centers is often accompanied by a depression of the pKa, bond dissociation free energy (BDFE), and/or hydricity (ΔG_{H-}) of one or more of the ligand's X-H bonds. This coordination-induced bond weakening is a ubiquitous phenomenon in synthetic, catalytic, and enzymatic processes and has been observed for a variety of coordination modes.¹ In extreme cases, as in the coordination of ammonia to Mo^I complexes, BDFEs can be depressed by up to 60 kcal/mol.²

In homogeneous electrocatalysis, the depression of X-H homolytic and heterolytic bond energies is crucial for accessing advantageous proton-coupled electron transfer (PCET) reactivities. Cooperative mediators often leverage the PCET behavior of weakened X-H bonds to shuttle proton and electron equivalents between a co-catalyst and the electrode.³ For instance, coordination of alcohol substrates to Cu^{II} depresses the β C-H BDFE, making it susceptible to hydrogen atom abstraction by 2,2,6,6-tetramethylpiperidine-*N*-oxyl TEMPO under oxidizing conditions.⁴ Ring protonation of decamethylcobaltocene affords a potent PCET donor that facilitates the Fe-mediated electroreduction of dinitrogen to ammonia.⁵ The Ru pyrimidazole complex Ru(2-(1H-imidazol-2-yl)pyridine)(acac)₂ **RuPyimH** can act as both 1e⁻/1H⁺ oxidant or reductant for intercepting or generating metal hydrides under electrocatalytic conditions because it has a very weak N-H bond.⁶⁻⁷

Despite the promising applications of the chemistry of ligation-weakened X-H bonds, a recent review of the subject by Boekell and Flowers notes that "relatively little work has been done to assess the underlying physical processes that give rise to coordination-induced bond weakening phenomena." As the popularity and scope of PCET-mediated strategies for electrocatalysis

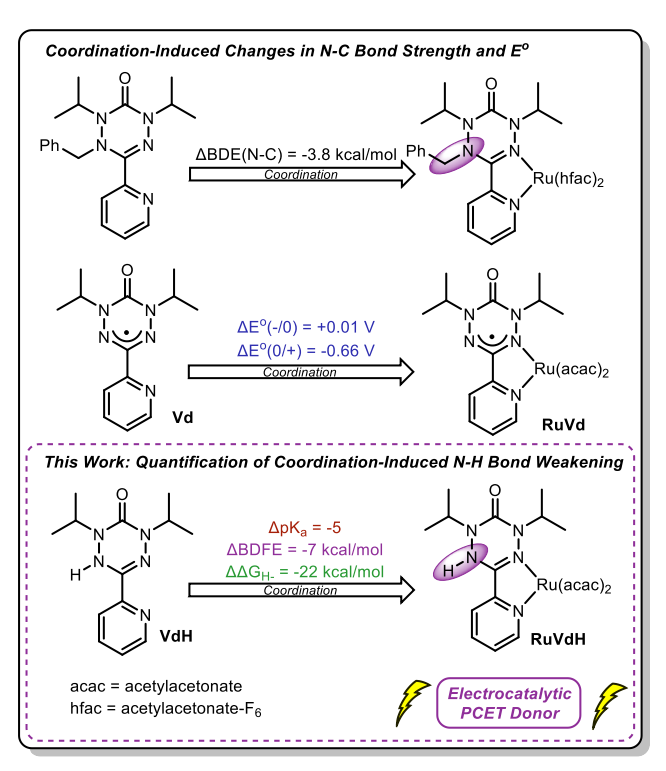


Figure 1. Coordination to Ru elicits changes in the thermochemistry of verdazyl ligands.

continue to expand, so does the motivation to understand the metal-ligand interactions that give rise to BDFE and hydricity depression. A recent study of RuPvimH and several related molecules characterized the thermochemistry of these compounds and discovered that the pKa and reduction potentials could be tuned independently through structural changes.⁸ Modifications to the acetylacetonate ligands altered the reduction potential, while variation of the substituents on the pyrimidazole itself had a greater effect on the N-H acidity. This study elucidates the factors that influence the N-H bond strength once the ligand is metalated, but the lack of thermochemical data for the uncoordinated pyrimidazole makes it difficult to discern what changes occur upon its binding to Ru^{II}.

We sought to interrogate the physical basis of coordination-induced bond weakening by directly comparing the

heterolytic and homolytic bond strengths of a ligand in both its free and metal-bound states. Verdazyl radicals and their metalated counterparts provide just such an opportunity. Verdazyls and metalloverdazyl complexes have principally been studied for their unique magnetic and electronic properties, but the weak N-H bonds of the corresponding leucoverdazyls make them interesting candidates as PCET reagents. Furthermore, coordination-induced changes in verdazyl reactivity have already been reported. An N-benzylated leucoverdazyl exhibits a 3.8 kcal/mol decrease in N-C bond dissociation enthalpy (BDE) upon coordination to Ru(hfac)₂ (Figure 1). While the free verdazyl Vd and its Ru(acac)₂-coordinated counterpart RuVd have very similar reduction potentials, the reduction potentials of the corresponding cations Vd+ and RuVd+ differ by 0.66 V (Figure 1). Previous studies of RuVd+ revealed significant mixing of the Ru and verdazyl orbitals, suggesting that reduction of this species is not a strictly ligand-centered nor metal-centered process. 15

Herein, we characterize the thermochemistry of both the leucoverdazyl **VdH** and its Ru(acac)₂-coordinated counterpart **RuVdH**. Electrochemical experiments reveal significant coordination-induced depression of the N-H pK_a, BDFE, and hydricity. DFT calculations were performed to elucidate the structural and electronic differences between the free and bound ligands, and they suggest that the bond weakening can in part be explained by the stabilization of the antiaromatic anionic **Vd**⁻ by the Ru center. PCET reactivity is observed for both compounds. Treatment of **Vd** with TEMPOH establishes a 1e⁻/1H⁺ transfer equilibrium. **RuVd** can electrocatalytically reduce a stable trityl radical by PCET, making it a rare example of an electrochemically-regenerable PCET reductant.^{3, 7, 16}

RESULTS AND DISCUSSION

Coordination-Induced N-H Bond Weakening

The cyclic voltammetry (CV) of both **RuVd** and **Vd** in MeCN have been reported previously. **Vd** has two reversible one-electron transfers at -1.36 and +0.20 V vs. Fc^{0/+}, which are attributed to the **Vd**-/0 and **Vd**^{0/+} couples. ¹⁴ **RuVd** has three fully reversible one-electron redox features at -1.35, -0.42, and +0.88 V vs. Fc^{0/+} corresponding to the **RuVd**-/0, **RuVd**0/+, and **RuVd**+/2+ couples, respectively. ¹⁵

To measure the pKa of RuVdH, RuVd titrated was with benzenesulfonamide (PhSO₂NH₂, $pK_a(MeCN) = 26.63^{17}$) in MeCN, and changes to the RuVd-10 couple were monitored by CV. At early titration points, the RuVd-/0 feature remains reversible but shifts to more positive potentials. As the PhSO₂NH₂ excess increases further, the outgoing reductive peak continues to shift positively, and the oxidative return feature decreases in magnitude. By the end of the titration, the feature becomes completely irreversible (Figure 2).

Assuming that electron transfer is fast relative to the voltametric scan rate, this behavior is consistent with 1e⁻/1H⁺ reduction of **RuVd** to **RuVdH** proceeding via an EC mechanism according to equations (1) and (2). This reaction transitions through the kinetic zones defined by Savéant, moving from DE (fully reversible) through KE (quasireversible) to zone KP (irreversible) as the favorability of proton transfer increases. The pseudo-first order equilibrium constant K_{EC} in equation (3) describes the ratio of **RuVd** and **RuVdH** at the electrode surface and is calculated directly from the apparent change

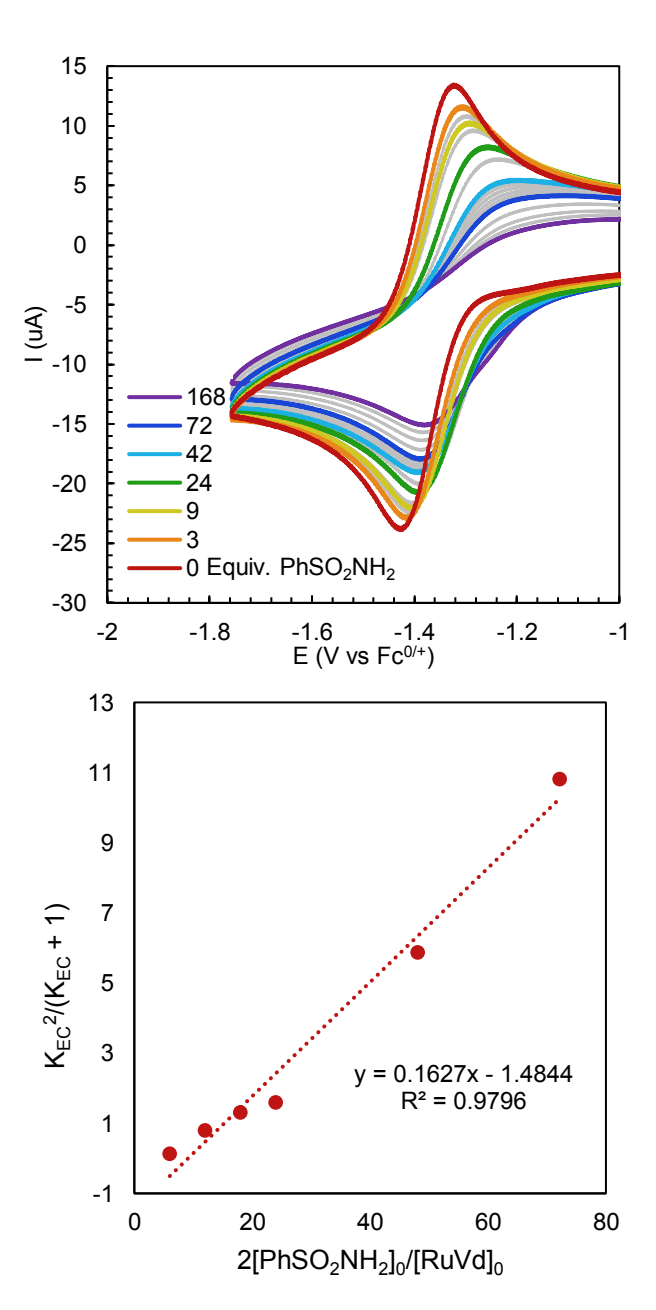


Figure 2. CV response of **RuVd** under acidic conditions. (Top) Titration of 1.5mM **RuVd** with PhSO₂NH₂ in 100 mM NBu₄PF₆ in MeCN, $\upsilon = 100$ mV/s. All scans were initially swept reductively. (Bottom) Determination of **RuVd**-/PhSO₂NH₂ proton transfer equilibrium constant by equation (4).

in E_{1/2}(RuVd^{0/-}) (ΔE) in zone DE.¹⁸ An equilibrium constant (K_{eq}) for the RuVd⁻/PhSO₂NH₂

proton transfer in equation (2) can then be calculated from K_{EC} as a function of the ratio of PhSO₂NH₂ to **RuVd** according to equation (4). A derivation of equation (4) is provided in the supplementary information.

$$RuVd + e \rightleftharpoons RuVd^{-} \tag{1}$$

$$RuVd^{-} + PhSO_{2}NH_{2} \rightleftharpoons RuVdH + PhSO_{2}NH^{-}, K_{eq}$$
 (2)

$$\frac{[RuVdH]}{[RuVd^{-}]} = K_{EC} = e^{\frac{F\Delta E}{RT}} - 1$$
 (3)

$$\frac{K_{EC}^2}{(K_{EC}+1)} = K_{eq} \left(\frac{2[PhSO_2NH_2]_0}{[RuVd]_0} \right)$$
 (4)

This affords a Keq of 0.1627 which corresponds to a **RuVdH** pKa of 26±1 (Figure 2).

Interestingly, the same gradual transition from reversible $1e^-$ reduction to irreversible $1e^-$ / $1H^+$ reduction can be achieved by varying the pK_a of the exogeneous acid instead of its concentration (See Supporting Information). With weaker acids (pK_a > 25), the reductive peak potential $E_{peak}(\mathbf{RuVd^{0/-}})$ remains relatively unperturbed at -1.40 V, but the oxidative return feature starts to disappear and shift to more positive potentials. With acids of medium strength ($22 < pK_a < 25$), $E_{peak}(\mathbf{RuVd^{0/-}})$ shifts positively up to -1.28 V, and the return feature disappears entirely. Acids as strong as salicylic acid (pK_a = 16.7) do not further alter the voltametric response. Notably, the $\mathbf{RuVd^{+/0}}$ feature remains unperturbed regardless of acid concentration or pK_a. This indicates that the loss of reversibility in the $\mathbf{RuVd^{-/0}}$ couple is not a result of decomposition of the complex and is instead dependent on the favorability of proton transfer to $\mathbf{RuVd^{-}}$. To confirm this, a scan rate study was performed on a solution of 1.2 mM \mathbf{RuVd} in the presence of 180 equiv. of PhSO₂NH₂(Figure S11). The plot of the peak anodic current for the $\mathbf{RuVd^{+/0}}$ feature vs. the square root of scan rate is highly linear, indicating that there is not significant decomposition of the reduced Ru species earlier in the scans (Figure S12). Decomposition would result in deviation from linearity at slower scan rates that give sensitive species more time to react.

The voltammetry of Vd in the presence of various acids was also examined, and a similar transition from $1e^-$ reduction to $1e^-/1H^+$ reduction was observed. Acids as weak as phenol $(pK_a=29.2 \text{ in MeCN})$ elicit a loss of reversibility in the $Vd^{0/-}$ feature and a positive shift in $E_{peak}(Vd^{0/-})$. This shift is fairly constant (~100 mV) for acids with pKas between 24.31 and 29.2, but decreasing the pKa further from 23.5 to 12.65 results in a dramatic positive shift of an additional 570 mV (Figure S17). This behavior is best explained by thermodynamic coupling of Vd reduction to the protonation of the ligand's pyridyl moiety. Such coupling is not observed for RuVd because the pyridyl lone pair is engaged in metallic bonding and is unavailable for protonation. Application of the pKa determination method from equations (1)-(4) to the titration of Vd with indole (pKa = 32.57 in MeCN) gives a pKa of 31 ± 1 for VdH.

The BDFEs and hydricities of both **RuVdH** and **VdH** can then be calculated according to equations (5) and (6),¹⁹⁻²⁰ and the complete thermochemical portraits of the metalated and free verdazyls are summarized by the square schemes in Figure 3.

$$BDFE(MeCN) = 1.364pK_a(RuVdH) + 23.06E^0(RuVd^{0/-}) + 52.6$$
 (5)

$$\Delta G_{H-}(MeCN) = 1.364pK_a + 23.06 \left(E^0 \left(RuV d^{0/-} \right) + E^0 \left(RuV d^{+/0} \right) \right) + 78.6 \tag{6}$$

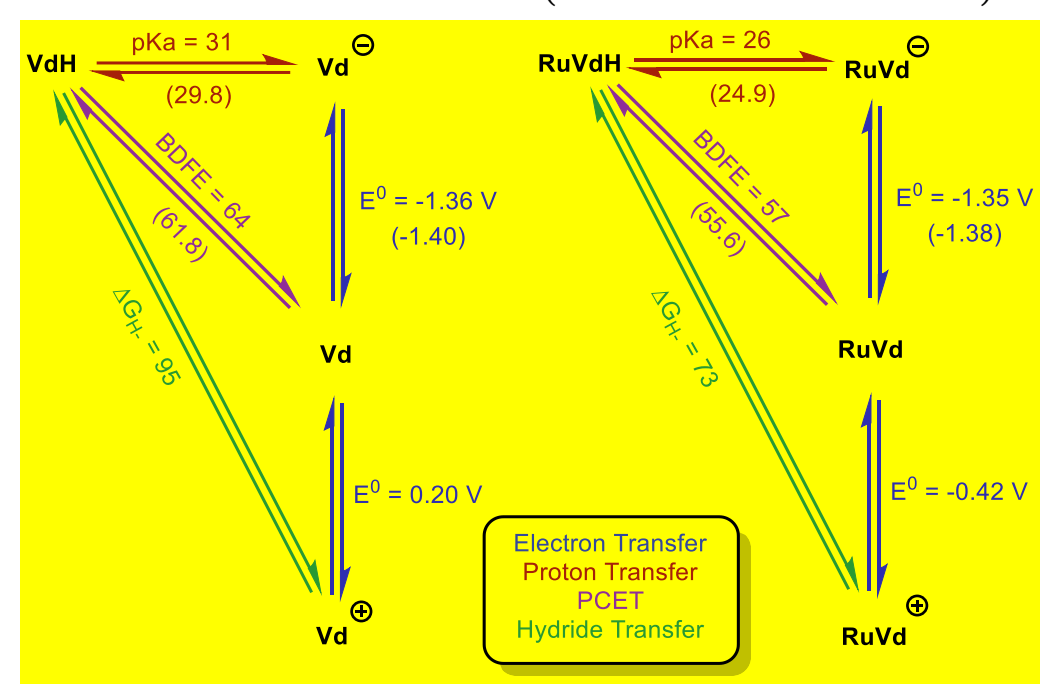


Figure 3. Thermodynamic Square Schemes for **Vd** and **RuVd** in MeCN. Reduction potentials are referenced to $Fc^{0/+}$ and BDFEs and hydricities are listed in kcal/mol. The uncertainties in the experimental pK_a measurements are ± 1 unit, and the uncertainties in the experimental BDFE and hydricity values are ± 1 kcal/mol. DFT values are listed in parentheses.

Table 1. Changes in Vd Thermochemistry upon coordination to Ru(acac)₂

Parameter	Δ (Coordination)
E°(+/0) (V)	-0.66
$E^{\circ}(0/-)(V)$	+0.01
pK_a	-5
BDFE (kcal/mol)	-7
$\Delta G_{\text{H-}}$ (kcal/mol)	-22

Overall, **RuVdH** is a potent PCET donor (BDFE = 57 ± 1 kcal/mol) and a mild hydride donor ($\Delta G_{H-} = 73\pm1$ kcal/mol). Table 1 enumerates the differences in **Vd** and **RuVd** thermochemistry from Figure 3, and these differences can be interpreted as the effects of coordination of **VdH** to Ru(acac)₂. Even though there is essentially no change in the potential of $E^{\circ}(0/-)$ for the two molecules,

 ${\bf RuVdH}$ is a considerably stronger reductant than ${\bf VdH}$ in terms of both PCET and hydride transfer capacity. The 0.66 V decrease in E $^{\circ}$ (+/0) is the principal contributor to the 22 kcal/mol decrease in N-H hydricity upon coordination. On the other hand, the 7 kcal/mol coordination-induced BDFE depression is entirely attributable to the decrease in N-H pKa.

The DFT-calculated²¹⁻²⁶ structures and frontier molecular orbitals shed light on the origin of this effect (Figures 4-5). Full computational details are available in the supplementary information. The average internal bond angle of the verdazyl C₂N₄ ring can be used as a measure

of the planarity of these rings (Figure 4). A planar six-membered ring has an average internal bond angle of 120°, whereas typical six-membered, monocyclic rings with one exo- and one endocyclic double bond have an average internal bond angle of 115-116°. ²⁷⁻²⁸ The SOMO and HOMO of **Vd** and **Vd**⁻ appear very similar; both are π -antibonding orbitals with two perpendicular nodes. However, the geometry of the two molecules

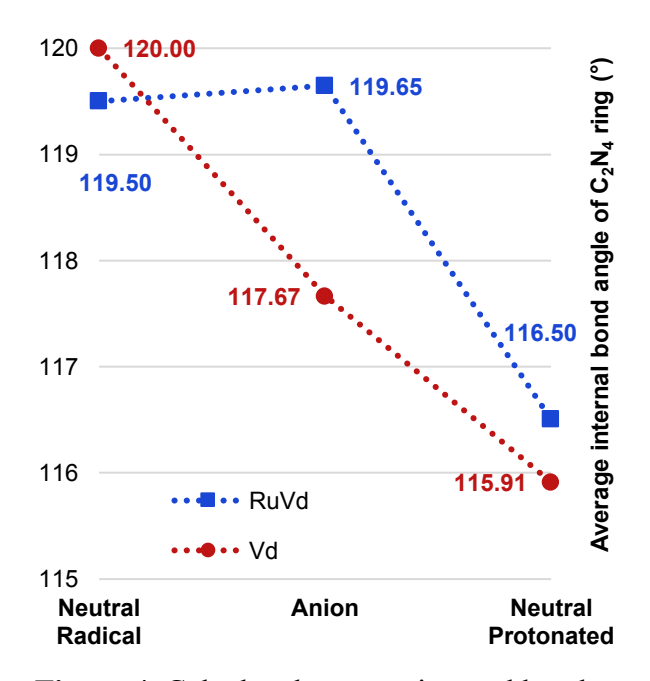


Figure 4. Calculated average internal bond angle of the verdazyl ring for RuVd, Vd, and their derivatives

is quite different (Figure 4). While the C_2N_4 ring of Vd is a $7\pi e^-$ non-aromatic system that is totally planar, the same ring in Vd^- distorts to avoid an $8\pi e^-$ antiaromatic condition. Protonation of Vd^- to VdH distorts the HOMO further, and the ring deplanarizes completely. Similar results are obtained when average normal deviation from the mean plane is used as the planarity metric instead of average internal bond angle (Figure S26-27).

The SOMO and HOMO of **RuVd** and **RuVd**⁻ are comprised of the π-antibonding orbitals from the ring and the out-of-phase d_{x2-y2} orbital from Ru. The C₂N₄ ring in the neutral radical shows only a slight deviation from planarity (Figure 4). However, unlike the uncoordinated **Vd**⁻, the anionic **RuVd**⁻ remains nearly planar. Protonation of the anion to **RuVdH** then results in near total deplanarization, similar to **VdH**. The HOMO of **RuVdH** is dominated by the Ru d_{z2}, with

minor contributions from the acac ligands. The relative planarity of the C_2N_4 ring in \mathbf{RuVd}^- in comparison to \mathbf{Vd}^- suggests that the Ru d_{x2-y2} plays a role in stabilizing the anionic ligand and alleviating antiaromaticity without distorting the ring. Stabilization of \mathbf{RuVdH} 's conjugate base therefore increases its thermodynamic acidity in comparison to \mathbf{VdH} .

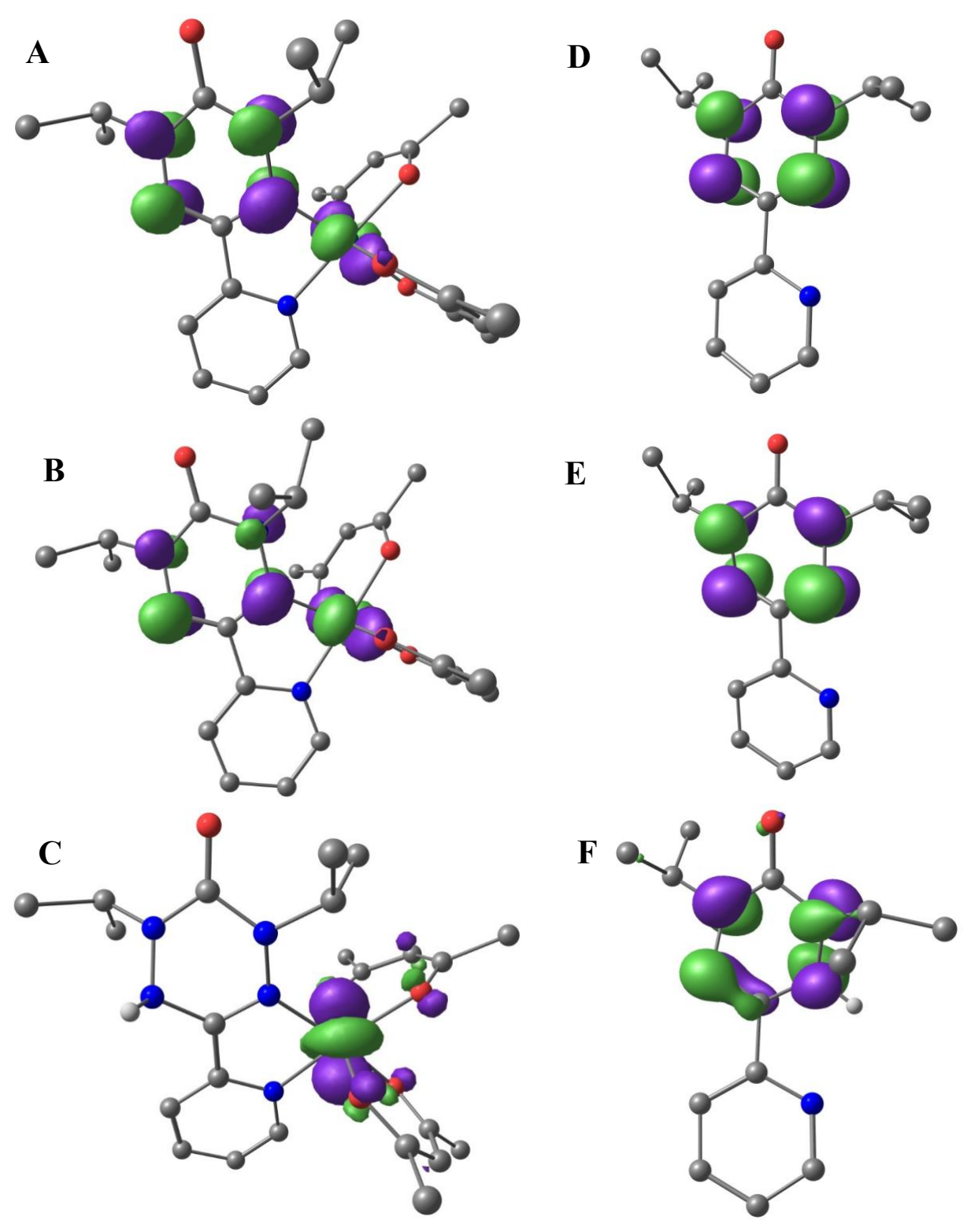


Figure 5. DFT-calculated frontier molecular orbitals. **RuVd** SOMO (A), **RuVd**⁻ HOMO (B), **RuVdH** HOMO (C), **Vd** SOMO (D), **Vd**⁻ HOMO (E), **VdH** HOMO (F). C-H bonds omitted for clarity.

Proton-coupled electron transfer behavior was observed for both the free and bound verdazyls. When **Vd** is treated with 1 equivalent of TEMPOH in MeCN-*d*₃, a PCET equilibrium is rapidly established, and a 1:5.4 ratio of **VdH** to TEMPOH is observed by ¹H NMR spectroscopy (See Supporting Information). Perturbation of the system by adding an equivalent of TEMPO radical establishes a new equilibrium. Based on a TEMPOH BDFE of 66.0 kcal/mol in MeCN,²⁹ this experiment gives a **VdH** BDFE of 64.0 kcal/mol, in excellent agreement with the value obtained through electrochemical experiments (Figure 3).

Observation of **RuVdH**'s PCET behavior proved challenging due to the instability of the reduced species **RuVd**- and **RuVdH**. Despite the well-behaved voltametric responses of these molecules, previous attempts to isolate **RuVdH** and the N-benzyl analog **RuVdBn** proved unsuccessful. ^{13, 30} We therefore returned to electrochemical methods to observe PCET reactivity.

Having previously observed electrocatalytic hydrogen atom transfer (HAT) processes for oxidative applications, 6,31 we anticipated that **RuVd** could act as a reductive PCET electrocatalyst. The persistent carbocation tris(p-tert-butylphenyl)carbenium hexafluorophosphate [CAr₃][PF₆] is a suitable acceptor substrate for demonstrating **RuVd**'s PCET reactivity. At the potentials required to generate **RuVdH**, [CAr₃][PF₆] is readily reduced to its corresponding trityl radical ·CAr₃. This persistent radical is then susceptible to further reduction to the triarylmethane HCAr₃ via PCET from **RuVdH** due to its greater homolytic bond strength (BDE(H-CAr₃) \sim 74 kcal/mol). Unlike the unsubstituted trityl radical ·CPh₃, ·CAr₃ does not undergo Gomberg dimerization due to its steric bulk, making it an ideal acceptor for the study of reductive PCET processes. 32

The insolubility of the ·CAr₃ radical in MeCN necessitated a switch to *o*-difluorobenzene (ODFB). Although slight changes in the reduction potentials of **RuVd** were observed in the new solvent (E°(**RuVd**-/0) = -1.58 V, E°(**RuVd**0/+) = -0.46 V, E°(**RuVd**+/2+) = +0.85 V vs Fc0/+ in ODFB), the CV of **RuVd** in the presence of acid was very similar in ODFB and MeCN (Figures 6 and S20-22). When treated with excess *p*-trifluoromethylbenzenesulfonamide (*p*-CF₃-PhSO₂NH₂ pK_a = 25.24 in MeCN) or acetic acid (pK_a = 23.5 in MeCN) in ODFB, the **RuVd**0/- feature loses reversibility and moves to a more positive potential. The **RuVd**+/0 feature remains fully reversible. [CAr₃][PF₆] exhibits two fully reversible reductive features (E°(CAr₃0/+) = -0.36 V, E°(CAr₃-/0) = -1.96 V vs Fc0/+ in ODFB). The addition of acetic acid does shift the CAr₃-/0 feature to more positive potentials, but not to the point that it fully overlaps the **RuVd** reduction with acetic acid. The normalized and overlayed voltammograms in Figure 6 suggest that, in the presence of acetic acid, **RuVd** can be reduced at a potential (-1.38 V) that will not reduce ·CAr₃, thus enabling the electrochemical regeneration of the PCET donor **RuVdH** in the presence of a persistent PCET acceptor.

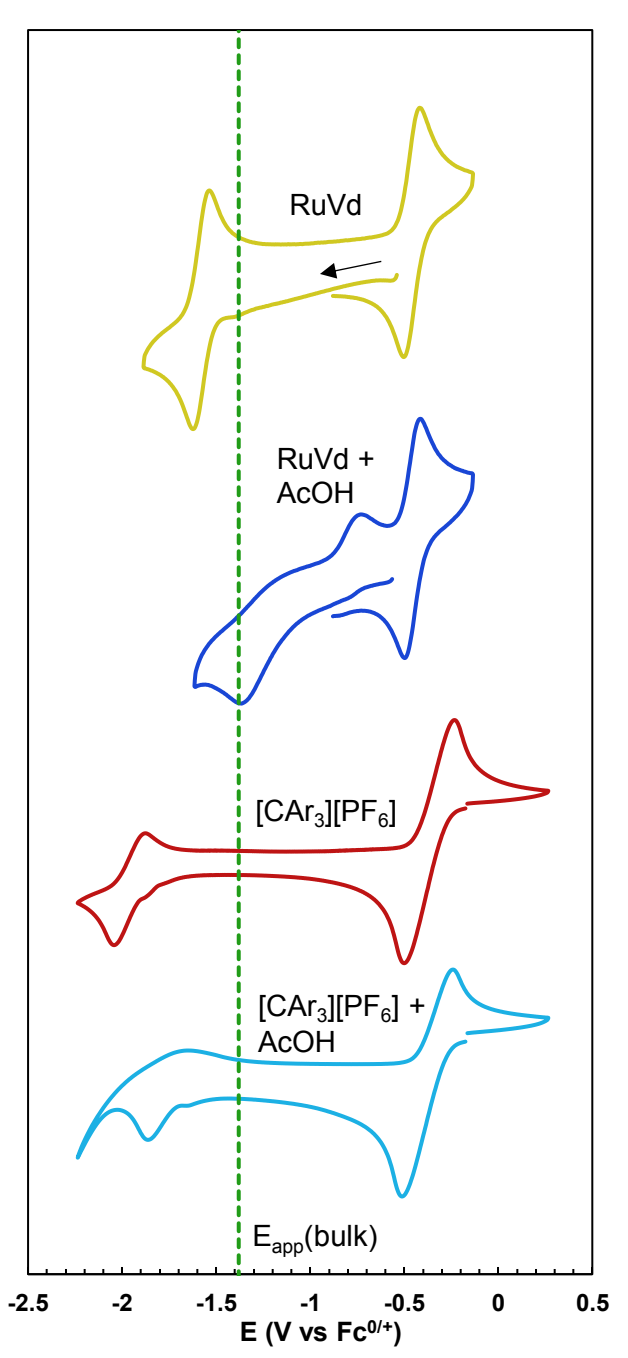


Figure 6. Normalized cyclic voltammetry of 0.5 mM **RuVd** in the absence (yellow) and presence (dark blue) of 42 mM acetic acid and of 11mM [CAr₃][PF₆] in the absence (red) and presence (light blue) of 42 mM acetic acid. (100 mM NBu₄PF₆ in ODFB, $\upsilon = 50$ mV/s). The green vertical line represents the applied potential of -1.38 V used in the bulk electrolysis experiments.

Indeed, bulk electrolysis at -1.38 V vs $Fc^{0/+}$ of 0.5 mM **RuVd** in the presence of excess [CAr₃][PF₆] and acetic acid results in the catalytic production of HCAr₃. Following the passage of 1.01 equivalents of electrons vs. [CAr₃][PF₆] substrate over 72 minutes, 6.5 turnovers of HCAr3 are recorded at a Faradaic efficiency (FE) of 59% (Figure 7). The remaining 41% of the passed charge is most likely contained in [CAr₃][PF₆] substrate that was reduced by the cathode to corresponding trityl radical, but was not reduced further before the electrolysis was ended. The control electrolysis, performed for the same duration at the same potential and substrate concentrations but with no RuVd, yields significantly less HCAr₃ at much worse efficiency (FE =12%) while passing 0.96 equivalents of electrons vs [CAr₃][PF₆]. This suggests that the majority of [CAr₃][PF₆] was converted to ·CAr₃ during this initial control electrolysis period. After the removal of the quantification aliquot, the reaction was spiked with 0.7 mM RuVd and electrolysis at -1.38 V was continued for an additional 72 minutes. For this second electrolysis period, 4.4 turnovers of HCAr₃ were produced at 80% Faradaic efficiency.

These experiments are consistent with the mechanism in Figure 8, wherein **RuVdH** acts as an electrocatalytic PCET donor. While we cannot rule out the possibility that **RuVdH** can also reduce CAr₃⁺ by hydride transfer (ΔG_H-(H-CPh₃) = 99 kcal/mol), the preparative electrolysis of [CAr₃][PF₆] to ·CAr₃ followed by catalytic production of HCAr₃ upon addition of **RuVd** indicates that **RuVdH** can access a 1e/1H⁺ reduction pathway. Although it is unclear whether PCET between **RuVdH** and ·CAr₃ is a stepwise or concerted process, it is apparent that **RuVdH** effects a 1e-/1H⁺ reduction that

the combination of acetic acid and a cathode cannot.

Figure 7. Bulk electrocatalytic reduction of [CAr₃][PF₆] by **RuVd** (top). Control electrolysis in the absence of **RuVd**, followed by **RuVd** spike and further catalysis (bottom).

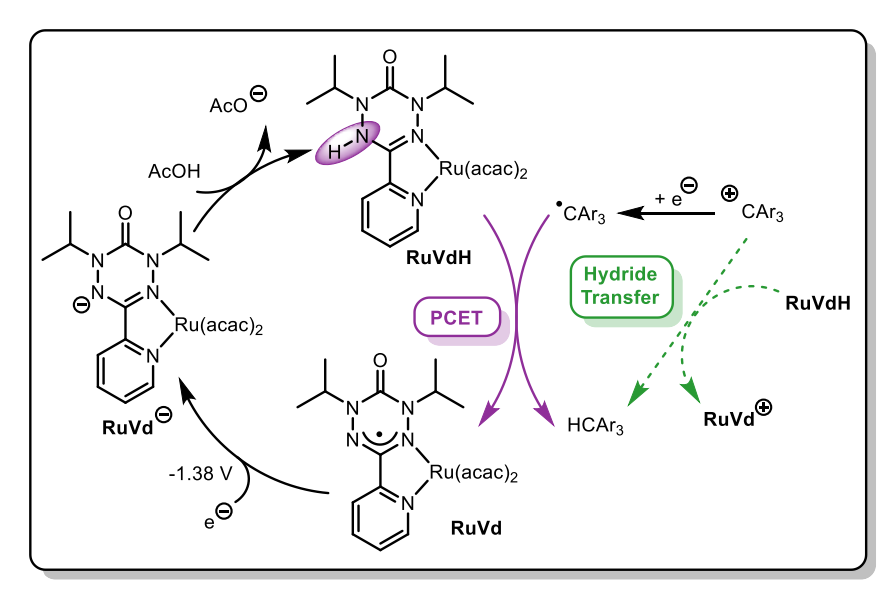


Figure 8. Proposed mechanism of electrocatalytic [CAr₃][PF₆] reduction to HCAr₃ via observed PCET (purple) and plausible hydride transfer (green) from **RuVdH**.

CONCLUSIONS

Coordination of the persistent radical Vd to the Ru(acac)₂ fragment results in significant depression of the heterolytic and homolytic N-H bond dissociation energies of the corresponding leucoverdazyl in MeCN. The 22 kcal/mol decrease in hydricity is mostly due to the -0.66 V difference between $E^{\circ}(\mathbf{RuVd^{0/+}})$ and $E^{\circ}(\mathbf{Vd^{0/+}})$. However, the 7 kcal/mol homolytic bond weakening is primarily driven by pK_a depression because $E^{\circ}(\mathbf{RuVd^{-/0}})$ and $E^{\circ}(\mathbf{Vd^{-/0}})$ are almost identical. DFT calculations suggest that the 5 pK_a unit depression is attributable to a stabilization of the $\mathbf{Vd^{-}}$ ligand in the conjugate base via mixing of the ligand π^* with the d_{x2-y2} of Ru. Whereas

the C_2N_4 ring of free Vd^- experiences significant deplanarization to avoid an $8\pi e^-$ antiaromatic condition, the coordinated Vd^- remains planar.

Proton-coupled electron transfer behavior is observed for both the free verdazyl and the Ru complex. Stoichiometric treatment of **Vd** with TEMPOH establishes a PCET equilibrium and affords a **VdH** BDFE that is in good agreement with the one obtained from voltammetric acid titration. **RuVd** can act as an electrocatalytic PCET reductant. It reduces a trityl radical to the corresponding triarylmethane via 1e⁻/1H⁺ transfer from **RuVdH**.

The metalated leucoverdazyl **RuVdH** is a rare example of an electrochemically-regenerable PCET donor with a BDFE lower than 60 kcal/mol.^{3, 29} Transition metal hydrides are often key intermediates in electrocatalytic reductions, and many of these intermediates have low BDFEs in this same <60 kcal/mol range.^{20, 33} **RuVdH** may therefore be able to mediate the formation of these metal hydride intermediates with near ergoneutrality. A close thermodynamic match between mediator and acceptor BDFE is desirable because a highly endergonic PCET might slow or halt catalysis, and a highly exergonic PCET may be a source of overpotential or introduce side reactivity in extreme cases. **RuVdH** and related complexes⁸ exhibiting coordination-induced bond weakening are therefore of great interest to the field of PCET-mediated electrocatalysis, which has experienced a surge of interest in recent years.^{5-7, 16, 31, 34} This work provides insight into the metal-ligand interactions behind coordination-induced bond weakening and underscores the importance of this phenomenon in the development of new electrocatalysts and electrocatalytic mediators.

SUPPORTING INFORMATION

Further experimental and computational details are available in the attached word document. The molecular coordinates of DFT-optimized structures have been compiled in an .xyz file.

AUTHOR INFORMATION

Corresponding Author

Robert M. Waymouth, Department of Chemistry, Stanford University, Stanford CA 94305, United States; orcid.org/0000-0001-9862-9509; Email: waymouth@stanford.edu

Authors

Conor M. Galvin, Department of Chemistry, Stanford University, Stanford CA 94305, United States; orcid.org/0000-0002-7678-5647

Daniel P. Marron, Department of Chemistry, Stanford University, Stanford CA 94305, United States; orcid.org/0000-0003-1588-768X

Julia M. Dressel, Department of Chemistry, Stanford University, Stanford CA 94305, United States; orcid.org/0000-0002-3601-9710

Notes

The authors declare no competing financial interest.

ACKNOWLEDGEMENTS

This study was based on work funded by the National Science Foundation (CHE-2101256). J.M.D. thanks the National Science Foundation for support in the form of a Graduate Research Fellowship (DGE-1656518). The authors would like to thank Professor David Brook (San Jose State University, Department of Chemistry) for sharing with us his expertise in verdazyl chemistry.

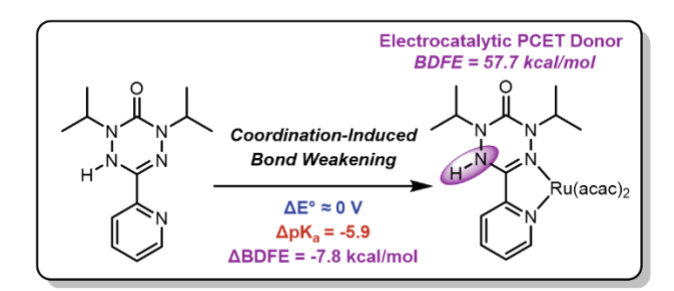
REFERENCES

- 1. Boekell, N. G.; Flowers, R. A., II, Coordination-Induced Bond Weakening. *Chemical Reviews* **2022**, *122* (16), 13447-13477.
- 2. Bezdek, M. J.; Guo, S.; Chirik, P. J., Coordination-induced weakening of ammonia, water, and hydrazine X–H bonds in a molybdenum complex. *Science* **2016**, *354* (6313), 730-733.
- 3. Reid, A. G.; Machan, C. W., Redox Mediators in Homogeneous Co-electrocatalysis. *Journal of the American Chemical Society* **2023**, *145* (4), 2013-2027.
- 4. Badalyan, A.; Stahl, S. S., Cooperative electrocatalytic alcohol oxidation with electron-proton-transfer mediators. *Nature* **2016**, *535* (7612), 406-410.
- 5. Chalkley, M. J.; Del Castillo, T. J.; Matson, B. D.; Peters, J. C., Fe-Mediated Nitrogen Fixation with a Metallocene Mediator: Exploring pKa Effects and Demonstrating Electrocatalysis. *Journal of the American Chemical Society* **2018**, *140* (19), 6122-6129.
- 6. McLoughlin, E. A.; Armstrong, K. C.; Waymouth, R. M., Electrochemically Regenerable Hydrogen Atom Acceptors: Mediators in Electrocatalytic Alcohol Oxidation Reactions. *ACS Catalysis* **2020**, *10* (19), 11654-11662.
- 7. Dey, S.; Masero, F.; Brack, E.; Fontecave, M.; Mougel, V., Electrocatalytic metal hydride generation using CPET mediators. *Nature* **2022**, *607* (7919), 499-506.
- 8. Groff, B. D.; Cattaneo, M.; Coste, S. C.; Pressley, C. A.; Mercado, B. Q.; Mayer, J. M., Independent Tuning of the pKa or the E1/2 in a Family of Ruthenium Pyridine–Imidazole Complexes. *Inorganic Chemistry* **2023**.
- 9. Brook, D. J. R., Coordination Chemistry of Verdazyl Radicals. *Comments on Inorganic Chemistry* **2015**, *35* (1), 1-17.
- 10. Koivisto, B. D.; Hicks, R. G., The magnetochemistry of verdazyl radical-based materials. *Coordination Chemistry Reviews* **2005**, *249* (23), 2612-2630.
- 11. Kunz, S.; Janse van Rensburg, M.; Pietruschka, D. S.; Achazi, A. J.; Emmel, D.; Kerner, F.; Mollenhauer, D.; Wegner, H. A.; Schröder, D., Unraveling the Electrochemistry of Verdazyl Species in Acidic Electrolytes for the Application in Redox Flow Batteries. *Chemistry of Materials* **2022**, *34* (23), 10424-10434.
- 12. Luo, Y.-R., *Comprehensive Handbook of Chemical Bond Energies*. 1st ed.; CRC Press: 2007.
- 13. Johnston, C. W.; Schwantje, T. R.; Ferguson, M. J.; McDonald, R.; Hicks, R. G., Metal coordination, and metal–ligand redox non-innocence, modulates allosteric C–N bond homolysis in an N-benzyl tetrazine. *Chemical Communications* **2014**, *50* (83), 12542-12544.

- 14. Gilroy, J. B.; McKinnon, S. D. J.; Koivisto, B. D.; Hicks, R. G., Electrochemical Studies of Verdazyl Radicals. *Organic Letters* **2007**, *9* (23), 4837-4840.
- 15. McKinnon, S. D. J.; Patrick, B. O.; Lever, A. B. P.; Hicks, R. G., Verdazyl radicals as redox-active, non-innocent, ligands: contrasting electronic structures as a function of electron-poor and electron-rich ruthenium bis(β -diketonate) co-ligands. *Chemical Communications* **2010**, 46 (5), 773-775.
- 16. Chalkley, M. J.; Garrido-Barros, P.; Peters, J. C., A molecular mediator for reductive concerted proton-electron transfers via electrocatalysis. *Science* **2020**, *369* (6505), 850-854.
- 17. Kütt, A.; Tshepelevitsh, S.; Saame, J.; Lõkov, M.; Kaljurand, I.; Selberg, S.; Leito, I., Strengths of Acids in Acetonitrile. *European Journal of Organic Chemistry* **2021**, *2021* (9), 1407-1419.
- 18. Saveant, J.-M. a. C., Cyrille, Coupling of Electrode Electron Transfers with Homogeneous Chemical Reactions. In *Elements of Molecular and Biomolecular Electrochemistry*, 2019; pp 81-181.
- 19. Warren, J. J.; Tronic, T. A.; Mayer, J. M., Thermochemistry of Proton-Coupled Electron Transfer Reagents and its Implications. *Chemical Reviews* **2010**, *110* (12), 6961-7001.
- 20. Wiedner, E. S.; Chambers, M. B.; Pitman, C. L.; Bullock, R. M.; Miller, A. J. M.; Appel, A. M., Thermodynamic Hydricity of Transition Metal Hydrides. *Chemical Reviews* **2016**, *116* (15), 8655-8692.
- 21. M. J. Frisch, G. W. T., H. B. Schlegel, G. E. Scuseria, M. A. Robb, J. R. Cheeseman, G. Scalmani, V. Barone, G. A. Petersson, H. Nakatsuji, X. Li, M. Caricato, A. Marenich, J. Bloino, B. G. Janesko, R. Gomperts, B. Mennucci, H. P. Hratchian, J. V. Ortiz, A. F. Izmaylov, J. L. Sonnenberg, D. Williams-Young, F. Ding, F. Lipparini, F. Egidi, J. Goings, B. Peng, A. Petrone, T. Henderson, D. Ranasinghe, V. G. Zakrzewski, J. Gao, N. Rega, G. Zheng, W. Liang, M. Hada, M. Ehara, K. Toyota, R. Fukuda, J. Hasegawa, M. Ishida, T. Nakajima, Y. Honda, O. Kitao, H. Nakai, T. Vreven, K. Throssell, J. A. Montgomery, Jr., J. E. Peralta, F. Ogliaro, M. Bearpark, J. J. Heyd, E. Brothers, K. N. Kudin, V. N. Staroverov, T. Keith, R. Kobayashi, J. Normand, K. Raghavachari, A. Rendell, J. C. Burant, S. S. Iyengar, J. Tomasi, M. Cossi, J. M. Millam, M. Klene, C. Adamo, R. Cammi, J. W. Ochterski, R. L. Martin, K. Morokuma, O. Farkas, J. B. Foresman, and D. J. Fox *Gaussian 09, Revision A.02*, Gaussian, Inc.: Wallingford, CT, 2016.
- Weigend, F., Accurate Coulomb-fitting basis sets for H to Rn. *Physical Chemistry Chemical Physics* **2006**, *8* (9), 1057-1065.
- 23. Weigend, F.; Ahlrichs, R., Balanced basis sets of split valence, triple zeta valence and quadruple zeta valence quality for H to Rn: Design and assessment of accuracy. *Physical Chemistry Chemical Physics* **2005**, *7* (18), 3297-3305.
- 24. Becke, A. D., Density-functional thermochemistry. III. The role of exact exchange. *The Journal of Chemical Physics* **1993**, *98* (7), 5648-5652.
- 25. Grimme, S.; Ehrlich, S.; Goerigk, L., Effect of the damping function in dispersion corrected density functional theory. *Journal of Computational Chemistry* **2011**, *32* (7), 1456-1465.
- 26. Marenich, A. V.; Cramer, C. J.; Truhlar, D. G., Universal Solvation Model Based on Solute Electron Density and on a Continuum Model of the Solvent Defined by the Bulk Dielectric Constant and Atomic Surface Tensions. *The Journal of Physical Chemistry B* **2009**, *113* (18), 6378-6396.

- 27. Cao, H.; Ma, S.; Feng, Y.; Guo, Y.; Jiao, P., Synthesis of β-nitro ketones from geminal bromonitroalkanes and silyl enol ethers by visible light photoredox catalysis. *Chemical Communications* **2022**, *58* (11), 1780-1783.
- 28. Li, X.-M.; Li, X.-M.; Lu, C.-H., Abscisic acid-type sesquiterpenes and ansamycins from Amycolatopsis alba DSM 44262. *Journal of Asian Natural Products Research* **2017**, *19* (10), 946-953.
- 29. Agarwal, R. G.; Coste, S. C.; Groff, B. D.; Heuer, A. M.; Noh, H.; Parada, G. A.; Wise, C. F.; Nichols, E. M.; Warren, J. J.; Mayer, J. M., Free Energies of Proton-Coupled Electron Transfer Reagents and Their Applications. *Chemical Reviews* **2022**, *122* (1), 1-49.
- 30. McKinnon, S. D. J.; Patrick, B. O.; Lever, A. B. P.; Hicks, R. G., Electronic Structure Investigations of Neutral and Charged Ruthenium Bis(β-diketonate) Complexes of Redox-Active Verdazyl Radicals. *Journal of the American Chemical Society* **2011**, *133* (34), 13587-13603.
- 31. Galvin, C. M.; Waymouth, R. M., Electron-Rich Phenoxyl Mediators Improve Thermodynamic Performance of Electrocatalytic Alcohol Oxidation with an Iridium Pincer Complex. *Journal of the American Chemical Society* **2020**, *142* (45), 19368-19378.
- 32. Eisenberg, D. C.; Lawrie, C. J. C.; Moody, A. E.; Norton, J. R., Relative rates of hydrogen atom (H.cntdot.) transfer from transition-metal hydrides to trityl radicals. *Journal of the American Chemical Society* **1991**, *113* (13), 4888-4895.
- 33. Waldie, K. M.; Ostericher, A. L.; Reineke, M. H.; Sasayama, A. F.; Kubiak, C. P., Hydricity of Transition-Metal Hydrides: Thermodynamic Considerations for CO2 Reduction. *ACS Catalysis* **2018**, *8* (2), 1313-1324.
- 34. Derosa, J.; Garrido-Barros, P.; Li, M.; Peters, J. C., Use of a PCET Mediator Enables a Ni-HER Electrocatalyst to Act as a Hydride Delivery Agent. *Journal of the American Chemical Society* **2022**, *144* (43), 20118-20125.

FOR TABLE OF CONTENTS ONLY:



SYNOPSIS: Coordination of a leucoverdazyl ligand to Ru significantly lowers the BDFE of the ligand's N-H bond. DFT calculations suggest that this coordination-induced bond weakening is in part caused by acidification of the N-H bond by stabilization of the anionic antiaromatic conjugate base by Ru. The Ru leucoverdazyl complex can act as an electrochemically-regenerable PCET donor in the reduction of a trityl radical to the corresponding triarylmethane.